R-matrix calculation of eigenchannel multichannel quantum defect parameters for strontium

J. Phys. B: At. Mol. Phys. **20** (1987) 4325-4345. Printed in the UK

R-matrix calculation of eigenchannel multichannel quantum defect parameters for strontium

M Aymar†, E Luc-Koenig† and S Watanabe‡

† Laboratoire Aimé Cotton, CNRS II, Bat. 505, 91405 Orsay Cedex, France
‡ Equipe de Recherche 261 du CNRS, Observatoire de Meudon-Paris, 92190 Meudon, France

Received 12 December 1986, in final form 27 March 1987

Abstract. Within the framework of the eigenchannel *R*-matrix method, theoretical calculations of the multichannel quantum defect (MQDT) parameters have been performed for $^{1,3}P^o$, $^{1,3}D^e$ and $^{1,3}S^e$ spectra of Sr. For the singlet spectra, both discrete and autoionisation regions below the Sr^+ 4d threshold are investigated, while the analysis of the triplets is restricted to the bound spectra below the Sr^+ 5s threshold. Near the Sr^+ 5s threshold, the calculated parameters are in good agreement with those previously fitted to spectroscopic data. The main improvements with respect to the empirical MQDT studies concern evidence of the large energy dependence of the parameters and identification of isolated perturbers of the $^1D_2$ and $^1S_0$ spectra. In addition, the energy levels and the spectral intensities are accurately reproduced and channel mixing and correlation effects in doubly excited states are analysed in detail. A close similarity is found between the 5s*n*p-4d*n*p $^1P^o$ mixing in Sr and the *ms*n*p*-*mp*n*s* $^1P^o$ mixing in the light alkaline earths Be and Mg. Such near invariance does not hold for the $^1D^e$ and $^1S^e$ spectra.

1. Introduction

Over the past decade there have been numerous theoretical studies on atomic doubly excited states, mainly for the simple two-electron systems He and H^- (see Fano (1983) and Fano and Rau (1986) for recent reviews). These works using hyperspherical coordinates, group theoretical approaches or molecular models have emphasised the important role played by the correlations between the two excited electrons. It is of particular interest to examine how the correlation effects seen in two-electron systems manifest themselves in doubly excited states of many-electron systems. Alkaline earths are good candidates for such studies, a wealth of experimental data being available. Analyses have been initiated for the light alkaline earths Be and Mg using the hyperspherical treatment and/or the *R*-matrix procedure (Lin 1983, Greene 1981, O'Mahony and Greene 1985, O'Mahony and Watanabe 1985, O'Mahony 1985). Though some authors have recently made steps toward elucidating dynamics of the correlation in heavier alkaline earths (Krause and Berry 1985), much remains to be understood.

A main difference between the two lightest alkaline earths and the heavier ones is that the first excited state of the lightest ions Be^+ and Mg^+ is the *n*p state whereas it is $(n-1)$d for the heavy alkaline-earth ions. This is expected to result in different correlation patterns between the light and heavy alkaline earths. In particular, one of the most interesting features in the spectra of heavy alkaline earths is the presence of many doubly excited states below the first ionisation limit, representing members of

0022-3700/87/174325+21$02.50

series converging to the $(n-1)$d or np ionisation limit. The autoionisation structure reflects the mixing of the $n\varepsilon l$ continua with doubly excited states. The interaction of doubly excited states and their associated Rydberg series with principal Rydberg series or continua should be viewed as the interaction between channels. Study of correlation effects in alkaline earths consists therefore in analysing channel coupling. The multichannel quantum defect (MQDT) approach is better suited than the configuration interaction method for studying correlation effects because it treats the short-range interactions and channel mixing using a small set of physical parameters.

The MQDT method of Seaton (1983) and Lu and Fano (Lu 1971, Lee and Lu 1973, Fano 1975) has been extensively used to analyse spectral data on alkaline earths. A concise description of the spectra was obtained using a small set of empirical parameters (see Aymar 1984 for a recent review). However, most of these studies are restricted to bound or autoionisation spectra just above the first threshold. Theoretical prediction of high-lying doubly excited states is of particular interest, necessitating, however, theoretical calculations of MQDT parameters. Although *ab initio* calculations have been previously carried out by Armstrong *et al* (1981) for some Rydberg series of Ca, Sr and Ba, additional investigations with increased precision and generality are desirable.

This paper aims at analysing channel coupling in Sr. For that purpose we use the eigenchannel R-matrix method presented by Greene (1983) and O'Mahony and Greene (1985). Specifically, we calculate the wavefunctions of the two electrons in the effective potential of the frozen Sr^{2+} core variationally within a finite volume V of the configuration space; by analytically joining them to Coulomb functions outside V, one obtains a reaction matrix, whose diagonalisation gives the energy-dependent theoretical MQDT parameters. This method has been successfully used to analyse channel coupling in Be and Mg (O'Mahony and Greene 1985, O'Mahony and Watanabe 1985, O'Mahony 1985). The extension to the heavier alkaline earths raises some problems: firstly, the number of interacting channels is larger; secondly, the $(n-1)$d wavefunction of the ion is known to be very sensitive to the electron-core interaction and the question is how to accurately describe this interaction; finally, the spin-orbit coupling becomes large.

Sr has been chosen for the following reasons.

(1) It is the heaviest alkaline-earth atom whose characteristics can be correctly reproduced without introducing spin-orbit coupling.

(2) *Ab initio* calculations, using the standard close coupling and/or configuration mixing approaches are even more scarce than in Ca and Ba; to our knowledge only a few excited energies have been calculated using the multiconfiguration Hartree-Fock (MCHF) method (Hansen and Persson 1977, Froese Fischer and Hansen 1981, Aspect *et al* 1984).

(3) Numerous empirical MQDT studies exist, but a recent comparison of MQDT and MCHF results (Froese Fischer and Hansen 1981) displayed some discrepancies, clearly showing that there are still unresolved problems.

This paper aims at giving a new insight into the electron correlations in Sr as well as answering questions previously raised in the literature which can be summarised as follows.

(1) The labelling of the low-lying perturbers of $^1S_0^e$ and $^1D_2^e$ spectra has created a controversy. The question is which of the two configurations $5p^2$ or $4d^2$ represents the perturber better (Armstrong *et al* 1979, Froese Fischer and Hansen 1981). In the same way the label $4d^2$ of the $^1D_2$ resonance observed by Esherick (1977) just above the Sr^+ 5s threshold remains to be verified.

(2) A two-channel MQDT model fitted to the energies and oscillator strengths of 5snp $^1P_1$ levels and of their perturber 4d5p was unable to reproduce the irregular behaviour of the continuous oscillator strengths of the autoionising lines 4d6p and 4d7p. What is the reason for this discrepancy?

(3) Systematic trends in alkaline earths have been previously discussed mainly for singlet spectra (Lu 1974, Wynne and Armstrong 1979, Greene 1981, O'Mahony and Greene 1985, O'Mahony 1985). Near invariance of the mixing between the two lowest channels msnp and mpns $^1P^o$ of light alkaline earths has been demonstrated; similar mixing between the msnp and $(m-1)$dnp $^1P^o$ channels of heavier alkaline earths was suggested by the empirical MQDT studies but remains to be checked by theoretical calculations. Regularities for $^1S^e$ and $^1D^e$ spectra of alkaline earths are less marked (Lu 1974, Wynne and Armstrong 1979, O'Mahony and Watanabe 1985, O'Mahony 1985). Are there any systematics for channel mixing in these spectra?

Section 2 describes the computational procedure. Section 3 presents the results obtained for the $^1P^o$, $^1D^e$ and $^1S^e$ and the corresponding triplet spectra of Sr. Section 4 summarises the results and suggests future directions. Atomic units are used throughout.

2. Computational procedure

The procedure consists of four steps. (i) The Schrödinger equation of the two-electron system outside a frozen core is solved within a finite reaction volume V of the configuration space using the non-iterative eigenchannel R-matrix method recently proposed by Greene (1983) and O'Mahony and Greene (1985). (ii) Outside the volume V, the solutions are joined to the Coulomb radial functions of dissociation channels and a reaction matrix K is obtained. (iii) Diagonalisation of this matrix K yields theoretical eigenchannel MQDT parameters and the corresponding eigenmodes. (iv) The Rydberg-state positions and absorption spectra are determined from the MQDT parameters using the standard procedure (Lu 1971, Lee and Lu 1973, Fano 1975). This procedure has been previously applied to analyse the effect of channel coupling in Be and Mg $^1P^o$ states (O'Mahony and Greene 1985) and in $^1D^e$ spectra of Be (O'Mahony and Watanabe 1985) and Mg (O'Mahony 1985). Only the fundamental points of the method are outlined below.

2.1. Non-iterative eigenchannel R-matrix method

The Schrödinger equation for the two electrons outside a closed-shell core is

$$H\Psi = (-\tfrac{1}{2}\nabla_1^2 - \tfrac{1}{2}\nabla_2^2 + U(r_1) + U(r_2) + 1/r_{12})\Psi = E\Psi \tag{1}$$

where the interaction of each valence electron with the core is represented by a local potential $U(r)$. Equation (1) may be written symbolically as

$$H\Psi = (-\tfrac{1}{2}\nabla^2 + U)\Psi = E\Psi. \tag{2}$$

Ψ is expanded in terms of basis functions y_k:

$$\Psi = \sum_k c_k y_k \tag{3}$$

where the superposition coefficients c_k are determined variationally. The choice of $U(r)$ and of the basis will be discussed in the next subsection. Equation (2) is equivalent to the normal logarithmic derivative defined by

$$(\partial/\partial n)\Psi + b\Psi = 0 \tag{4}$$

on the boundary surface S of the volume V, where b is

$$b = \int_V [-\nabla\Psi^* \cdot \nabla\Psi + 2\Psi^*(E-U)\Psi]\,\mathrm{d}V \left(\int_S \Psi^*\Psi\,\mathrm{d}S\right)^{-1}. \tag{5}$$

The variational principle leads to $\partial b/\partial c_k = 0$, equivalently to an eigenvalue problem for b in the vector space of the coefficients c_k, namely

$$\boldsymbol{\Gamma c} = b\boldsymbol{\Lambda c} \tag{6}$$

where

$$\Gamma_{kl} = \int_V [-\nabla y_k \cdot \nabla y_l + 2y_k(E-U)y_l]\,\mathrm{d}V \tag{7}$$

stems from the Hermitian part of the Hamiltonian matrix and

$$\Lambda_{kl} = \int_S y_k y_l\,\mathrm{d}S \tag{8}$$

is the surface overlap matrix.

The eigenvalues b_β and eigenvectors $\Psi_\beta(\boldsymbol{r}_1, \boldsymbol{r}_2)$ for a preselected value of the total energy E are simply the eigenvalues and eigenstates of the R matrix, which are closely related to the two-electron normal modes due to electronic correlations (O'Mahony and Greene 1985, O'Mahony and Watanabe 1985).

2.2. Model potential and basis set

We exploit a simple model potential to represent the electron–closed-shell-core interaction in Sr^+, namely

$$U(r) = -r^{-1}[2 + 36\exp(-\alpha_1 r) + \alpha_2 r\exp(-\alpha_3 r)] \tag{9}$$

where the parameters α_i ($\alpha_1 = 3.4675$, $\alpha_2 = 2.6357$, $\alpha_3 = 1.0078$) are adjusted so that the eigenvalues of the one-electron radial equation

$$[-\tfrac{1}{2}\mathrm{d}^2/\mathrm{d}r^2 + l_1(l_1+1)/2r^2 + U(r) - \varepsilon_{n_1 l_1}]\Phi_{n_1 l_1}(r) = 0 \tag{10}$$

coincide with the experimental energies of the low-lying 5s, 5p and 4d levels of Sr^+.

In this work we neglect the spin–orbit interaction and represent Ψ in the LS coupling scheme, expanding it as a superposition of independent-particle functions y_k (equation (3))

$$\Psi(\boldsymbol{r}_1, \boldsymbol{r}_2) = \mathscr{A} \sum_{nl_1 ml_2} c^{l_1 l_2}_{nm} \Phi_{nl_1}(r_1) F^{nl_1}_{ml_2}(r_2)\, Y_{l_1 l_2 LM}(\hat{r}_1, \hat{r}_2)(\chi_{s_1}(1)\chi_{s_2}(2))^{SM_S} \tag{11}$$

where $\mathscr{A}$ denotes the antisymmetriser and the two-electron spherical harmonics and spin functions are defined in the standard manner.

In expansion (11) the indices nl_1l_2 define a specific channel converging to the Sr^+ nl_1 threshold. The Φ_{nl_1} radial functions describing the Sr^+ orbitals are necessarily enclosed within the reaction volume V. In contrast, the $F^{nl_1}_{ml_2}$ functions pertain to the outermost

electron, thus having a non-vanishing probability on the surface S when it escapes. The radial basis functions $\Phi_{nl_1}F^{nl_1}_{ml_2}$ are chosen to represent the motion of the two electrons flexibly in the whole configuration space. Consequently two sets of basis functions are included in expansion (11). The first one is designed to describe the asymptotic region where one electron is far from the core, $r_1 \gg r_2$ or $r_2 \gg r_1$. The second set of basis functions is chosen to describe the highly correlated motion in the reaction region where both electrons are at about equal distances from the core, i.e. $r_1 \sim r_2$. In this region, the mutual screening leads to the expansion of the inner electronic orbital and the contraction of the outer one as well as to minimisation of the bielectronic repulsion by favouring the angular position $\hat{r}_1 = -\hat{r}_2$. This angular correlation is described by the superposition over l_1 and l_2 in equation (11). The second set of functions describes the short-range interactions between the two electrons and therefore the corresponding functions are forced to vanish on the surface S.

As discussed by Greene (1983) and O'Mahony and Greene (1985) the number of solutions of equation (6) equals the number of open or weakly closed channels having non-negligible amplitude on the surface S. Therefore this number is entirely determined by the first set of basis functions. The introduction of the second set of basis functions does not increase the number of solutions; these additional channels are referred to as strongly closed channels. Our final analysis to be presented in § 3 shows that the strongly closed channels are very important for representing perturbers of Rydberg series. A model restricted to N open or weakly closed channels, employed for demonstrating the effect of strongly closed channels, will be referred to as a restricted N-channel model.

Consider more precisely the construction of basis functions, starting with the asymptotic region. A radial basis function consists of Φ_{nl_1} representing a Sr^+ orbital and $F^{nl_1}_{ml_2}$ describing the Rydberg or continuum electron. In this work the functions Φ_{nl_1} are determined by solving equation (10) and forcing their amplitudes to vanish on the boundary surface S. Φ_{nl_1} thus represents a Sr^+ orbital accurately only when this orbital is contained well within the volume V so that the true orbital function has an exponentially small amplitude at the surface. This specific connection between the size of the target state and that of V plays an important role in choosing the radius r_0 for the spherical volume V. The Rydberg or continuum functions $F^{nl_1}_{ml_2}$ are obtained by solving the single-electron radial equation for $Sr^+ + e^-$, approximating the bielectronic interaction by the monopole potential (Cowan 1981) created by the inner electron. Following O'Mahony and Greene (1985) we impose two kinds of boundary conditions on $F^{nl_1}_{ml_2}$.

A first set of orthogonal orbitals is obtained by solving the Schrödinger equation with the condition that each orbital vanishes on the boundary $r = r_0$. This set is complemented by a second one obtained by integrating the single-electron Schrödinger equation at several different energies which yields non-zero values of the orbitals and a variety of logarithmic derivatives on the boundary. Let us note in passing that the $F^{nl_1}_{ml_2}$ orbitals of the second kind are neither orthogonal to one another, nor orthogonal to the orbitals with zero amplitude at $r = r_0$. The non-orthogonality adds flexibility to the y_k basis but can lead to numerical inaccuracies when the basis becomes overcomplete. We have found it important to keep orbitals of the second kind to as few as possible. An open or weakly closed channel is well described by six orbitals of the first kind and three of the second.

Consider now the basis set introduced to describe the reaction region. The valence electron of Sr^+ can polarise and relax in response to the outermost electron, which

represents a major part of the core relaxation in the present model, the Sr^{2+} core being treated as frozen. This effect is known to be particularly important for the 4d orbital in Sr (which occupies a position immediately next to the second row of transition elements in the periodic table) (Griffin *et al* 1969, Connerade *et al* 1980); the potential barrier associated with the centrifugal term $l(l+1)/r^2$ also has a considerable influence on how the 4d orbital contracts and thus on the description of electron–closed-shell interaction. Basis functions $\phi_{4d'} F^{4d'}_{ml_2}$, where the relaxed 4d′ orbital is obtained by solving the radial equation for the neutral Sr, are introduced to supply the necessary flexibility to describe the different terms where the 4d electron is less tightly bound than in Sr^+. The radial functions $F^{4d'}_{ml_2}$ actually satisfy the same equation as before, namely the single-electron radial equation for $Sr^+ + e^-$, and are forced to vanish on S.

Another short-range effect arises from the coupling with the strongly closed channels converging to excited thresholds and associated with larger values of l_1 and l_2. Let us emphasise that due to the boundary condition on the surface S, the corresponding radial functions Φ_{nl_1} cannot be associated with target states of Sr^+ since they are forced to have negligible amplitude outside the reaction region. A strongly closed channel is described by five orbitals all vanishing on S.

Final results must not depend on the choice of the reaction radius r_0, which however needs to be large enough to enclose the charge distribution of Sr^+ nl_1. However, as stressed by O'Mahony and Greene (1985), numerical accuracy improves rapidly when r_0 is chosen to be as small as possible. An accurate description of series converging to the Sr^+ 5s, 4d and 5p thresholds is obtained with $r_0 = 14$ au; it must be emphasised that an identical result is obtained with $r_0 = 15$ au.

2.3. *Theoretical MQDT parameters*

Outside V the outer electron moves in a Coulomb potential if we neglect terms decreasing faster than r^{-3} (permanent quadrupole moment, polarisation potential, ...); thus its wavefunction is described by a superposition of the energy-normalised regular and irregular Coulomb functions f and g (Greene *et al* 1979, Seaton 1983). The R-matrix eigenchannel function Ψ_β corresponding to the eigenvalue b_β may be projected onto a Sr^+ ionic state represented by Φ_i yielding

$$\langle \Phi_i \| \Psi_\beta \rangle = f_i(\varepsilon_i, r_0) I_{i\beta} - g_i(\varepsilon_i, r_0) J_{i\beta} \tag{12a}$$

$$-b_\beta \langle \Phi_i \| \Psi_\beta \rangle = (\partial/\partial r) f_i(\varepsilon_i, r_0) I_{i\beta} - (\partial/\partial R) g_i(\varepsilon_i, r_0) J_{i\beta} \tag{12b}$$

where the double bar means surface integration over S leaving behind only the radial degree of freedom of the outermost electron. ε_i is the electron energy relative to the ionisation limit of the ith channel. The coefficients $I_{i\beta}$ and $J_{i\beta}$ are determined by solving the linear system (12).

The reaction matrix is defined by

$$\boldsymbol{K} = \boldsymbol{J}\boldsymbol{I}^{-1}. \tag{13}$$

We obtain theoretical values for the eigenchannel MQDT parameters $\tan \pi\mu_\alpha$ and $U_{i\alpha}$ (Lee and Lu 1973, Fano 1975) by diagonalising $\boldsymbol{K}$. Let us note that the orthogonal matrix $U_{i\alpha}$ represents the transformation between the dissociation channels i, described in the pure LS coupling scheme, and the close-coupling eigenchannels α.

Spectral intensities can be analysed with the MQDT parameters and the dipole matrix elements $\tilde{D}_\beta$ between the ground state and the R-matrix eigenchannels. The representation with respect to the MQDT eigenchannels is accomplished by (O'Mahony and

Greene 1985)

$$D_\alpha = \sum_{\beta i} \tilde{D}_\beta (\boldsymbol{I}^{-1})_{\beta i} U_{i\alpha} \cos \pi \mu_\alpha . \tag{14}$$

In this work a configuration mixing calculation including the s^2, p^2, d^2 and f^2 configurations was performed to obtain the ground-state wavefunction and energy (-0.619 au). Dipole matrix elements D_α were calculated using the length and velocity formulations and convergence was checked by comparing the two results. For $\varepsilon < 0$, the f and g diverge exponentially as r increases, giving a source of numerical error during the matching operation. It is in order to overcome this difficulty that the strongly closed channels are distinguished from other channels and their functions are confined entirely in V. According to Seaton (1983) the use of f and g is best restricted to energies such that $\varepsilon > -1/(2l^2)$. For energies lower than $-1/(2l^2)$ the channels should be treated as strongly closed in order to bypass the matching operation.

2.4. MQDT analyses

Although the MQDT parameters may be obtained by a theoretical calculation such as ours, most of the previous studies aimed at analysing experimental data with the aid of the empirically determined MQDT parameters. The empirical procedure often fitted the parameters to a particular spectral range. Being weakly dependent on energy, they were extrapolated in order to analyse other spectral ranges. Extrapolations often assumed the μ_α to be constant or linearly dependent on energy and the $U_{i\alpha}$ to be constant except for some cases like the Ba $^1P^o$ spectrum (Armstrong *et al* 1979). This type of study will be hereafter referred to as the 'empirical MQDT' analysis.

The $^{1,3}P^o$, $^{1,3}D^e$ and $^1S^e$ spectra of Sr have been previously studied using the empirical procedure (Lu 1977, Esherick 1977, Armstrong *et al* 1979, Wynne and Armstrong 1979, Beigang and Schmidt 1983). A full exposition of how to describe discrete and autoionising spectra using the eigenchannel MQDT parameters can be found in various papers (Lu 1971, Lee and Lu 1973, Fano 1975); only the essential points are outlined here.

Below the first ionisation limit, for each energy level $\tilde{E}$ one defines effective quantum numbers ν_i for each ionisation limit I_i through the relation

$$\tilde{E} = I_i - R/\nu_i^2 . \tag{15}$$

Here the energies $\tilde{E}$ and the ionisation limits I_i are referred to the Sr ground state and R is the Rydberg constant for Sr ($\tilde{E}$, I_i and R are in cm^{-1}). Bound-state energy levels represented by a set of ν_i ought to satisfy equation (15) and the following relationship simultaneously:

$$\det |F_{i\alpha}(\nu_i, \mu_\alpha)| = 0 \tag{16a}$$

where

$$F_{i\alpha}(\nu_i, \mu_\alpha) = U_{i\alpha} \sin \pi(\nu_i + \mu_\alpha). \tag{16b}$$

Equation (16a) ensures the exponential decline of the bound-state wavefunctions. The graphical representation exploited by Lu and Fano (Lu 1971, Lee and Lu 1973) consists of plots of $-\nu_i$ against ν_j for chosen pairs of effective quantum numbers. We shall concentrate on the Lu-Fano plot of ν_s and ν_d and on their relationship $-\nu_s = f(\nu_d)$ implied by equation (16a). Here ν_s is referred to the ionisation energy $I_{5s} = 45\,932.19\ cm^{-1}$ and ν_d to the average of the Sr^+ 4d levels, i.e. $I_{4d} = 60\,656.29\ cm^{-1}$.

Calculation of the spectral features for continuum states necessitates the imposition of appropriate boundary conditions as well as normalisation of the continuum wavefunctions (Lee and Lu 1973). Generally we impose the collision eigenchannel boundary condition on open channels, namely

$$\det |F_{i\alpha}(-\tau, \mu_\alpha)| = 0 \tag{17}$$

whereby the open-channel functions all have the same phaseshift τ asymptotically. There are as many solutions as the open channels. In this work there is only one solution because the autoionisation spectrum below the Sr^+ 4d threshold consists of one open channel 5sεl and several closed channels. The graph $\tau = f(\nu_d)$ is the direct extension of the Lu–Fano plot $-\nu_s \pmod 1 = f(\nu_d)$ to the above-threshold energy range.

We performed the MQDT analysis using a modified form of the MQDT code of Robaux and Aymar (1982) taking into account the energy dependence of the parameters.

3. Results

We shall now present the results for the $^1P^o$, $^1D^e$ and $^1S^e$ spectra and the corresponding triplet spectra. The study of the singlet spectra is carried out in the discrete and autoionising range below the Sr^+ 4d threshold whereas the analysis of the triplet states is restricted to the discrete spectra.

3.1. $^1P^o$ spectrum

Extensive experimental data have been obtained for the $^1P^o$ spectrum. Our purpose is to re-analyse, with the aid of the *R*-matrix MQDT parameters, the experimental data on level positions (Moore 1952, Garton and Codling 1968), oscillator strengths from the ground state (Parkinson *et al* 1976) and continuum oscillator strengths in the autoionising spectral range below the Sr^+ 4d threshold (Hudson *et al* 1969). Several empirical MQDT analyses were devoted to this spectrum (Lu 1977, Esherick 1977, Armstrong *et al* 1979). On the one hand a two-channel model was previously found to be sufficient to describe the perturbation of the principal 5snp $^1P^o$ series by the 4d5p $^1P^o$ perturber; on the other hand it proved incapable of reproducing the profiles of the 4d6p and 4d7p $^1P^o$ autoionising lines (Lu 1977). We shall account for this problem.

Below the first ionisation limit the spectrum consists of the two channels 5snp and 4dnp, whereas above the threshold additional channels 4dnf, 5pns and 5pnd have to be accounted for. We shall focus our attention mainly on the 5snp and 4dnp channels and disregard the spin–orbit interaction which affects the 4dnf levels (Garton and Codling 1968) but not the ones of interest.

We shall present successively a two-channel analysis of the discrete and autoionising spectra and a five-channel study of the above-threshold range.

3.1.1. Two-channel model. Let us describe first through the example of the $^1P^o$ spectrum how the convergence of the MQDT parameters depends on the strongly closed channels. In the first step we only included configurations of the type 5snp and 4dnp in the expansion (11). This gives two quantum defects μ_1 and μ_2 and one mixing angle θ pertaining to the orthogonal matrix $\boldsymbol{U}$. This calculation shows that the two channels

mix over a wide energy range but it does not achieve close agreement with the experimental data; in particular the value of μ_2 appears too small, indicating that the perturber 4d5p is located too high. It is thus necessary to include other configurations. The core relaxation is taken into account by including the configurations 4d′*n*p and 4d′*n*f. The configurations 4d*n*f, 5p*n*s and 5p*n*d describe those channels which are strongly closed below the Sr^+ 5s threshold. For comparison with previous empirical MQDT studies, the present two-channel model has been extended above threshold by ensuring, even in this range, that the *n*f, *n*s and *n*d orbitals in 4d*n*f and 5p*nl* have zero amplitude at $r = r_0$.

Table 1 shows the configurations introduced in our calculation and their influence on the MQDT parameters at the Sr^+ 5s threshold. The first row corresponds to the restricted two-channel model involving a basis limited to nine orbitals of the 5s*n*p configuration and nine of the 4d*n*p configuration. For the other rows, each additional configuration is described by five orbitals with zero amplitude at $r = r_0$. Notice that the inclusion of additional configurations always increases the quantum defects, in agreement with the known theorem (Hahn *et al* 1962, Percival 1960) that introducing more closed coupled channels always increases the phaseshifts. The particularly noticeable effect of the 5p*n*s on the μ_2 parameter is analogous to that found in light alkaline earths such as Be and Mg. The mixing between the *m*s*n*p and *m*p*n*s channels is usually very large (Greene 1981, O'Mahony and Greene 1985). The influence of the 4d′*n*p and 4d′*n*f configurations on the μ_2 value is also in agreement with the conclusions drawn by Froese Fischer and Hansen (1985) on Ca. The inclusion of the core relaxation lowers the energy of the *m*d(*m*+1)p $^1P^o$ level ($m = 3$ in Ca and 4 in Sr).

Table 1. Two-channel MQDT parameters for the $^1P^o$ spectrum at the Sr^+ 5s threshold.

Number of orbitals	Configurations added to 5s*n*p and 4d*n*p	This work			Previous works			
		μ_1	μ_2	θ/π	μ_1	μ_2	θ/π	Reference
18	0	0.820	0.310	0.180				
23	4d*n*f	0.828	0.417	0.210				
33	4d*n*f+5p*n*s+5p*n*d	0.867	0.436	0.195	0.926	0.494	0.203	Lu (1977)
43	4d*n*f+5p*n*s+5p*n*d +4d′*n*p+4d′*n*f	0.872	0.478	0.205	0.892	0.490	0.195	Armstrong *et al* (1979)
					0.94	0.67	0.21	Armstrong *et al* (1981)

Figure 1 is a plot of the MQDT parameters showing their specific energy dependence. The most striking feature is the close similarity between our curve representing the variation of the mixing angle θ between the 5s*n*p and 4d*n*p channels and the curves previously obtained by O'Mahony and Greene (1985) for the angle θ describing the *m*s*n*p-*m*p*n*s mixing in Be ($m = 2$) and Mg ($m = 3$): θ rises from no mixing at low energy to approximately equal mixing ($\theta \sim \pi/4$) at higher energies. This behaviour is tightly connected with the correlation phenomenon arising from the potential ridge found for fixed $R = \sqrt{r_1^2 + r_2^2}$ at $r_1 = r_2$, as emphasised by the earlier hyperspherical studies of doubly excited states of He (Lin 1974, Macek 1966). Since both the potential energy term and the kinetic energy operator have a well defined symmetry with respect to the ridge, so does the eigenfunction. This symmetry manifests itself noticeably in the reaction region, where the kinetic energy of the two electrons exceeds the potential

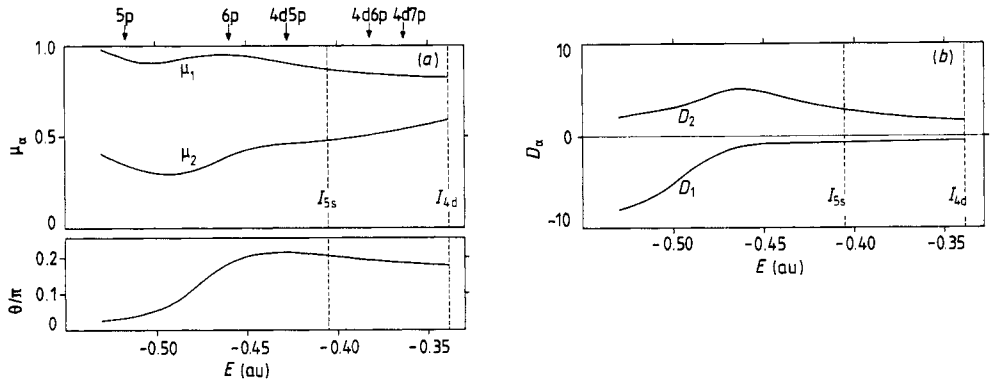

Figure 1. MQDT parameters for the $^1P^o$ spectrum in the two-channel analysis as functions of the energy E relative to the double ionisation threshold: (a) eigenquantum defects μ_1 (5snp), μ_2 (4dnp) and mixing angle θ; some experimental levels are indicated by vertical arrows (np means 5snp); (b) dipole matrix elements using the velocity form.

energy; they can thus exchange both radial kinetic energy and angular momenta freely. The radial correlation pattern is characterised by Lin's index $A = '+'$ or $'-'$ (Fano 1983, Lin 1974, Watanabe and Lin 1986) whereas the angular correlation pattern is characterised by Herrick's (K, T) quantum numbers (Herrick *et al* 1980, Ezra and Berry 1983 and references therein). In any event, strong radial and angular correlations are described by the relaxed radial orbitals and the mixing of higher angular momenta ($l_1 l_2$) with the low ones (Cavagnero 1984). In the present case this fact leads to the mixing of the 4d'np, 4dnf, 4d'nf, 5pns and 5pnd channels with the 5snp and 4dnp ones. The short-range interaction which prevails in the reaction zone determines the asymptotic form of the close-coupling eigenstates specified by the mixing angle θ. Which channel is more important depends on the degree of quasidegeneracy of the various channels with different ionisation thresholds.

Let us note in passing that the fairly large mixing is a signature of strong correlations, the equal mixing corresponding to the largest possible. In many systems, such as alkaline earths, nearly equal mixing occurs (Greene 1981, O'Mahony and Greene 1985, Fano 1983) as was suggested by the empirical MQDT analyses of the lowest $^1P^o$ channels msnp and ($m-1$)dnp in Ca, Sr and Ba (Wynne and Armstrong 1979, Armstrong *et al* 1979). The theoretical verification of this equi-partition rule in Sr is a key result of our calculation.

Comparison of the R-matrix parameters obtained in this work with the MQDT parameters fitted to experimental data (table 2) shows that our values are a little smaller, indicating that our final basis is probably too limited. Nevertheless, our theoretical MQDT parameters give a much better description of experimental energies than those previously obtained by Armstrong *et al* (1981) using the local density approximation.

Now let us consider the Lu-Fano plot of the discrete $^1P^o$ spectrum displayed in figure 2 as well as the energy and quantum defects for some particular levels given in table 2. It is clear that our theoretical energy levels agree well with experimental ones. Even the lowest 5s5p $^1P^o$, always disregarded by the empirical MQDT studies, is accurately described; good representation of this level is possible only by taking into account the large energy dependence of the MQDT parameters.

Table 2. Comparisons of our calculated energies and quantum defects with some observed values. The quantum defects μ are calculated with respect to the Sr^+ 5s or 4d limit. Experimental energies are from Moore (1952), Esherick (1977) and Beigang *et al* (1983) (energies $\tilde{E}$ in cm^{-1} are referred to the Sr ground state).

	This work		Experiment		
Level	$\tilde{E}$	μ	Level	$\tilde{E}$	μ
^1P					
5s5p	21 665	2.873		21 698	2.872
4d5p	41 205	2.625		41 172	2.627
Limit		2.686			2.730
^3P					
			$^3P_0$	14 317	3.136
5s5p	13 926	3.148	$^3P_1$	14 504	3.131
			$^3P_2$	14 899	3.119
			$^3P_0$	37 292	2.833
4d5p	37 164	2.839	$^3P_1$	37 302	2.832
			$^3P_2$	37 337	2.831
^3D					
			$^3D_1$	18 159	2.012
5s4d	18 466	2.000	$^3D_2$	18 218	2.010
			$^3D_3$	18 319	2.006
			$^3D_1$	35 007	1.831
5s5d	35 319	1.784	$^3D_2$	35 022	1.828
			$^3D_3$	35 045	1.825
			$^3D_1$	44 854	1.911
5s12d	44 871	1.832	$^3D_2$	44 860	1.882
			$^3D_3$	44 865	1.858
^3S					
5s6s	29 190	3.440		29 039	3.451
5s7s	37 540	3.384		37 424	3.408
5s8s	40 806	3.373		40 761	3.393
Limit		3.347			3.37

Let us now turn to our results on oscillator strengths. The dipole matrix elements calculated from the dipole velocity and the dipole length are very similar. Thus we present results obtained from the velocity form only. The D_1 parameters (figure 1(b)) shows a large energy dependence as in the case of the 2s*n*p close-coupling channel of Be (O'Mahony and Greene 1985). The large value of D_2 over a wide energy range, including the domain where the channel mixing is weak, results from the non-negligible $4d^2$ component in the ground-state wavefunction.

The oscillator strength distribution in the discrete spectrum is often renormalised in such a way as to compare with the oscillator strength density in the autoionisation range (Lu 1971, Lee and Lu 1973). The results presented below have all been renormalised in this fashion. In figure 3 we compare the oscillator strength densities calculated with the two-channel model (figure 3(*a*)) with the experimental data (figure 3(*c*)). The oscillator strength data are from Parkinson *et al* (1976); the densities of oscillator strength in the continuum are extracted from the curves published by Hudson *et al* (1969); only the wider resonances associated with $^1P^o$ levels are reported in figure 3(*c*); the positions of some other $^1P^o$ levels are indicated by vertical arrows. The insets

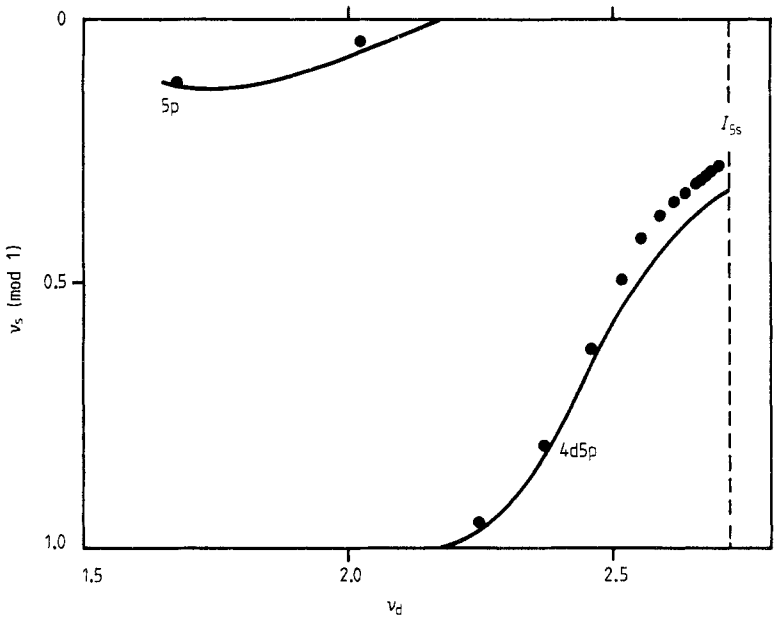

Figure 2. Lu–Fano plot of the $^1P^o$ spectrum: ——, theoretical curve; ●, experimental levels (Moore 1952, Garton and Codling 1968) (np means 5snp).

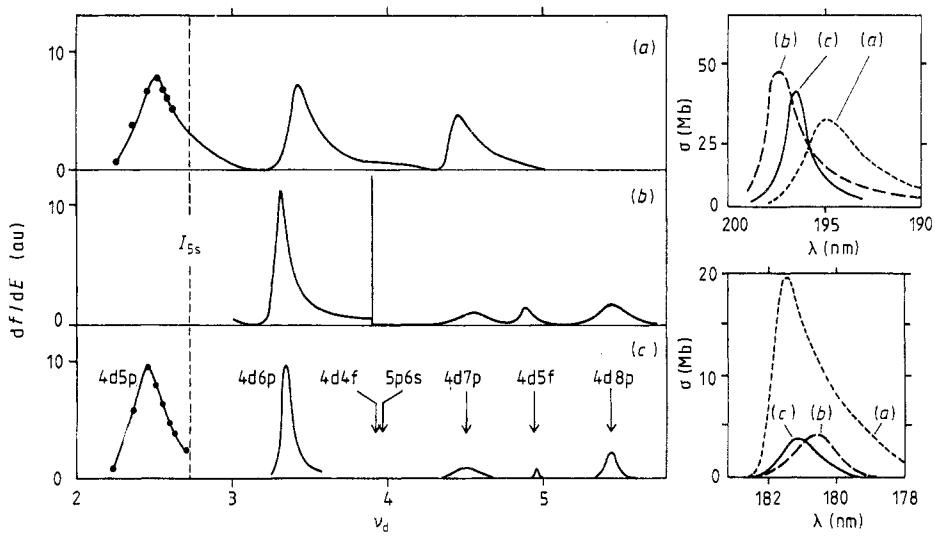

Figure 3. Oscillator strength density for the $^1P^o$ absorption spectrum from the ground state as a function of the effective quantum number ν_d. The theoretical values obtained by either the two-channel (a) or five-channel model (b) are compared with experimental results (Parkinson *et al* 1976, Hudson *et al* 1969) (c). Insets (at right) present absorption cross sections, obtained using the above models (a) and (b) or the results (c), in the wavelength range corresponding to the 4d6p and 4d7p resonances.

give details for the 4d6p and 4d7p resonances; here the cross section is plotted against the wavelength.

Below the Sr^+ 5s ionisation threshold our prediction reproduces the width and intensity of the renormalised experimental oscillator strengths well. However, a large departure between experiment and theory occurs above threshold: the calculated df/dE for 4d6p has a larger width than the experimental profile and the calculated 4d7p line is too intense (see the insets). Similar discrepancies were found by Lu (1977) using MQDT parameters fitted to experimental data relevant to the discrete spectrum. These are due to the limitation of the two-channel treatment, as we have now verified.

3.1.2. Five-channel model. In order to explain the irregular behaviour of 4dnp $^1P^o$ resonances as n increases, a five-channel calculation has been performed. The 4dnf, 5pns and 5pnd channels are now treated as weakly closed and nf, ns and nd orbitals with non-zero amplitude at $r = r_0$ are added to the previous basis set (table 1). This model is restricted to the above-threshold range because below I_{5s} one has $\varepsilon < -1/(2l^2)$ for the 4dnf channel with $l = 3$.

We found that all five channels are mixed and that inclusion of the mixing considerably improves the description of the 4d6p and 4d7p resonances: the 4d6p resonance becomes sharper while the 4d7p resonance broadens (see insets).

Strong admixture of the 5pnd and 5pns characters is found in all the resonances. Among the numerous resonances observed in the experimental absorption spectrum below the Sr^+ 4d threshold (Garton and Codling 1968, Garton *et al* 1968, Hudson *et al* 1969), only one structure has been previously ascribed to a 5pnl $^1P^o$ level, namely the 5p6s, but no structure was identified as 5p5d. Our five-channel model predicts the existence of two interfering resonances close to the experimental positions of the 4d4f and 5p6s levels; one resonance can be unambiguously ascribed to a 4d4f level but the other corresponds in fact to a 5p6s + 5p5d level. No other level assignable to a 5pnl level was found below the 4d8p $^1P^o$ level. The detailed structure of the 4d5f resonance is not satisfactorily reproduced even though the position appears reliable.

3.2. $^1D^e$ spectrum

The even parity $J = 2$ discrete spectrum has been observed and analysed by Esherick (1977) using the empirical MQDT method. Breakdown of the strict *LS* coupling scheme, owing to the spin-orbit interaction, is evident for highly excited 5snd $^1D_2$ and $^3D_2$ levels. This breakdown is characterised by an avoided crossing of the two series near $n \simeq 15$, 16 followed by an interchange in the spin character. Spin-orbit interaction being disregarded in this work, the $^1D_2$ and $^3D_2$ series cross and no information on the singlet-triplet mixing can be obtained. Nevertheless, with regard to energies, the spin-orbit interaction affects only a limited number of levels and the calculated energies can be compared with the experimental ones; however, above the crossing, the $^1D_2$ series must be compared with the experimental energies of $^3D_2$ (Esherick 1977) and *vice versa.*

The principal Rydberg series 5snd $^1D_2$ is affected by two perturbers. The influence of the 4d6s level is distributed over many high members of the principal series, none of which can be properly identified as 4d6s. Another low-lying level at 36361 cm^{-1}, referred to as P in the following, affects the 5s5d and 5s6d levels. It has been labelled as $5p^2$ in the literature and treated in the empirical MQDT studies (Esherick 1977, Wynne and Armstrong 1979) as the lowest level of a series converging to the Sr^+ 5p

limit. However, MCHF calculations performed by Froese Fischer and Hansen (1981) and by Aspect *et al* (1984) showed that such a single-particle label is inadequate. Taking into account the interaction between the $5p^2$ and $4d^2$, the perturber P was found to have the $4d^2$ component two times more than the $5p^2$ component. A new analysis of this spectrum is thus of particular interest to resolve the controversy. The even-parity autoionisation spectrum remains largely unknown; two lines have been assigned to the $^1D_2$ spectrum, namely the 4d5d (Newsom *et al* 1973) and a resonance just above the Sr^+ 5s threshold ($\bar{E} = 46\,380\ cm^{-1}$) tentatively identified as $4d^2$ by Esherick (1977) which will be referred to as P′ in this work. Here again confirmation of the assignment is worthwhile.

A four-channel model (5s*n*d, 4d*n*s, 4d*n*d, 5p*n*p) is used here to analyse the $^1D^e$ spectrum. Here again, additional configurations describing strongly closed channels (5p*n*f and 4d*n*g) and core relaxation terms (4d′*n*s and 4d′*n*d) are included in the basis expansion. All these configurations, except for the 4d*n*g, were found to have a non-negligible influence on the MQDT parameters.

The variation of the eigenquantum defects with energy is displayed in figure 4(*a*). The four channels are strongly mixed over all of the energy range studied. The predominant asymptotic channel, labelled by i in each close-coupling channel α, depends strongly on the energy; this point is illustrated in figure 4(*a*) by distinguishing for each channel α the channel i corresponding to the maximum value of $U_{i\alpha}$. The avoided crossings, observed at $E = -0.44$, -0.415 and -0.40 au interchange i labels for some α channels. Channel mixing is thus strongly energy dependent. For instance, the mixing of channel 5s*n*d with either 4d*n*d or 5p*n*p is large over the whole range studied, the 5s*n*d–4d*n*d mixing being stronger than the 5s*n*d–5p*n*p one below the Sr^+ 5s threshold; the situation reverses above the threshold. The 5s*n*d–4d*n*s mixing varies more regularly as the energy increases: it increases rapidly, reaches a maximum at threshold and then decreases slowly.

This four-channel model allows us to reproduce all of the experimental data, as shown in figure 4(*b*) which displays $-\nu_s \pmod 1 = f(\nu_d)$ below the Sr^+ 5s threshold and $\tau = f(\nu_d)$ above the threshold. (See also table 3.) The rise of the phaseshift just

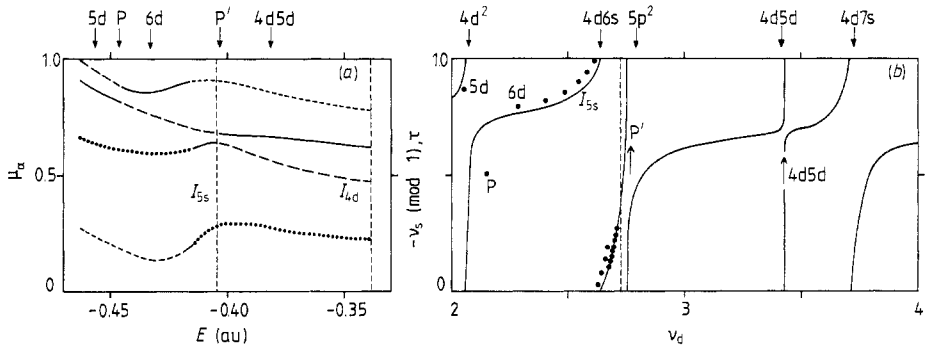

Figure 4. $^1D^e$ spectrum. (*a*) MQDT eigenquantum defects as functions of the energy E relative to the double ionisation threshold: ——, 5s*n*d; · · · · ·, 4d*n*s; - - -, 5p*n*p; — —, 4d*n*d (see text); some experimental levels are indicated by vertical arrows (*n*d means 5s*n*d). (*b*) Lu–Fano plot: ——, theoretical curve $-\nu_s = f(\nu_d)$ or $\tau = f(\nu_d)$; ●, experimental bound levels (Moore 1952, Esherick 1977); vertical arrows in the middle indicate observed autoionising levels (Esherick 1977, Newsom *et al* 1973); vertical arrows at the top indicate the theoretical $5p^2$ and 4d*nl* levels.

Table 3. Comparison of some $^1D_2$ energy levels calculated by different MQDT models with experimental values (energies in cm^{-1} are referred to the Sr ground state).

Level	Three channels: 5s*n*d, 4d*n*s and 4d*n*d		Three channels: 5s*n*d, 4d*n*s and 5p*n*p		Four channels: 5s*n*d, 4d*n*s, 4d*n*d and 5p*n*p		Experiments' previous label	
P	40 819	$4d^2$	43 514	$5p^2$	36 165	$4d^2$	36 961	$5p^2$
4d6s†	46 500	$>I_{5s}$	45 296	5s15d	44 594	5s11d	44 578	5s11d
P′					46 200	$5p^2$	46 380	$4d^2$
4d5d	51 660	4d5d			51 350	4d5d	51 356	4d5d

† Since the 4d6s level is spread out over many Rydberg levels, the 5s*n*d level given in this row corresponds to the level where the admixture of the 4d6s $^1D_2$ configuration reaches the maximum.

above the threshold perfectly describes the resonance P′ observed by Esherick (1977); similarly the 4d5d resonance is well located. Below the threshold our interpretation of the 4d6s perturbation is in perfect agreement with the results of Esherick (1977). The 4d6s level is found to be spread out over many 5s*n*d levels with a maximum admixture of 3.5% in the 5s11d level, to be compared with the 5% admixture found by Esherick (1977). Though the description of the lower perturber P is less accurate, the deviation between experimental and theoretical energies for P($\sim 800\ cm^{-1}$) is smaller than that ($\sim 2000\ cm^{-1}$) given by the MCHF calculation of Aspect *et al* (1984).

Turning to the labelling of the P and P′ perturber, our result for the P perturber is in perfect agreement with the MCHF prediction. The P level is found to have a d^2 component twice as large as the p^2 one. Although the single-particle label is not adequate for P and P′, it appears to be better to reverse the labels previously given in the literature, identifying P as the $4d^2\ ^1D_2$ level and P′ as the $5p^2\ ^1D_2$.

We now wish to comment on the possibility of reproducing the experimental data with a three-channel model, as previously done by Esherick (1977). We carried out two different three-channel calculations corresponding to the neglect of either the 5p*n*p or the 4d*n*d channel. Neither of them is capable of reproducing the experimental data as shown in table 3. Both calculations badly reproduce the perturbation of high-lying levels and the low-lying level P. Clearly the $4d^2$ and $5p^2$ levels strongly repel each other to give a low-lying $4d^2$ level and an autoionising $5p^2$ one. These treatments support the remarks of Froese Fischer and Hansen (1981) concerning the limits of empirical MQDT fit: when only one level of a perturbing series is known, the empirical MQDT analysis is unable to identify the perturber and additional information is needed. This point has been previously discussed by Wynne and Armstrong (1979) and Aymar *et al* (1980). The MQDT parameters fitted to experimental data strongly depend on the assumptions on which the MQDT model is based and lose their physical meaning.

Our final comment concerns comparison of the electron correlations in Sr $^1D^e$ with those in light alkaline-earth atoms Be $^1D^e$ and Mg $^1D^e$ and in Al $^2D^e$. The sd-pp coupling in these elements has been previously analysed (O'Mahony and Watanabe 1985, O'Mahony 1985) using the same eigenchannel *R*-matrix procedure. A great similarity was found between Mg and Al, while the behaviour of Be turns out to be different. A main difference between the light alkaline earths and the heavier one lies in the existence of $(n-1)dnl$ channels converging to the $(n-1)d$ threshold lower than the np one. The presence of the large pp-dd mixing in heavy alkaline earths results in a different sd-pp coupling and the striking similarity between the sp-ps $^1P^o$ mixing in light alkaline earths and the sp-dp $^1P^o$ mixing in heavier ones does not hold for $^1D^e$

spectra (Wynne and Armstrong 1979). Moreover, the evolution with atomic number Z of the phaseshift for the d wave considerably differs from its evolution for s and p waves (Manson 1969); this also results in less striking evidence for the systematics of the $^1D^e$ alkaline earths.

3.3. $^1S^e$ spectrum

The $^1S^e$ spectrum presents some similarities with the $^1D^e$ one, namely the principal Rydberg series $5sns\ ^1S_0$ is perturbed by a low-lying level located between $n=6$ and 7; the identification of this perturber, labelled $5p^2\ ^1S_0$ in the literature, is also a matter of controversy, as in the $^1D_2$ case. MCHF calculations of Froese Fischer and Hansen (1981) and of Aspect *et al* (1984) predicted that both the $4d^2$ and $5p^2$ components have nearly equal weights in the perturber denoted P. The $^1S_0$ spectrum was analysed by Escherick (1977) using a two-channel empirical MQDT model ($5sns$, $5pnp$), but later Wynne and Armstrong (1979) showed that a fit of the same quality can be obtained using a different two-channel model ($5sns$, $4dnd$) and they concluded that additional information is necessary to decide which label is the most appropriate one.

We performed a three-channel calculation ($5sns$, $5pnp$, $4dnd$) of the $^1S_0$ spectrum to reproduce the experimental data of Moore (1952) and Esherick (1977). Configurations describing the strongly closed channels $4fnf$ and $5gng$ and the core relaxation terms $4d'nd$ have been included in the expansion (11). The quantum defects are found to be almost independent of these additional configurations in the low-energy range but strongly dependent on the $4fnf$ and $4d'nd$ between the Sr^+ 5s and Sr^+ 4d thresholds. The variation of the eigenquantum defects with energy, displayed in figure 5(a), is very large mainly for the $4dnd$ channel. The coupling of the channel $5sns$ with either $5pnp$ ot $4dnd$ is very weak in the whole discrete energy range, considerably smaller than the analogous coupling in the $^1D^e$ spectrum. This situation is quite similar to that occurring in the light alkaline earths Be and Mg where the ss-pp mixing is weaker than the sd-pp mixing (Lu 1974). Above the Sr^+ 5s threshold, ss-pp coupling is stronger than ss-dd, mainly near the avoided crossing at $E=-0.375$ au. With regard to the pp-dd mixing, this mixing is stronger than in the $^1D^e$ spectrum above the Sr^+ 5s threshold, but weaker below.

The variation of $-\nu_s$ (or τ) with ν_d is displayed in figure 5(b). Here again μ_1 is slightly too small to reproduce the experimental quantum defects perfectly. The theoretical P level (36398 cm^{-1}) deviates from the experimental one (37 160 cm^{-1}); however, here again, the deviation (approximately 800 cm^{-1}) is smaller than that obtained by the MCHF calculation (approximately 2300 cm^{-1}). In both $^1S_0$ and $^1D_2$ cases the perturber is too low in energy. However, the correct order of the $^1D_2$ and $^1S_0$ perturbers is well reproduced, whereas it was inverted in the MCHF calculation (Aspect *et al* 1984).

As far as the $5p^2$ or $4d^2$ character is concerned, no definitive conclusion can be drawn from our study; in fact, due to the weakness of the coupling of the channel $5sns$ with the perturbing channels, the wavefunction of the P level is extremely sensitive to very small change of the MQDT parameters. This extreme sensitivity was not found in the $^1D^e$ spectrum. Different trials corresponding to different basis sets as well as different values of r_0 were thus needed; they led to the conclusion that the $4d^2$ character is here also predominant. For completeness we have searched for the $5p^2$ (or $4d^2$) above the Sr^+ 5s threshold. We found a sharp rise of the phaseshift near the predicted 4d6d resonance which manifests itself in the $5pnp$ channel. However, in the absence

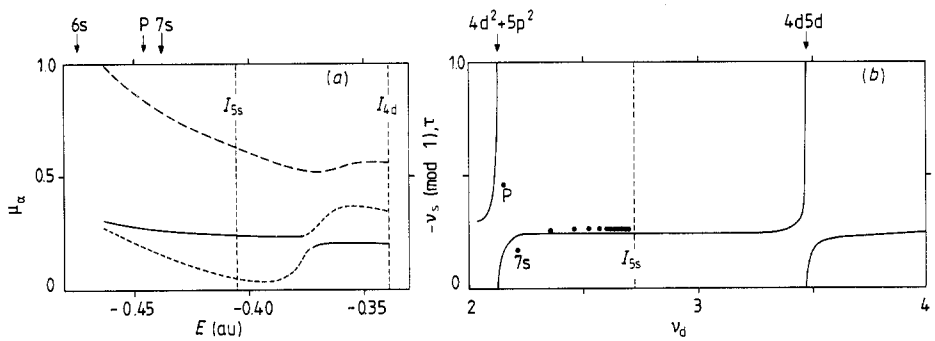

Figure 5. $^1S^e$ spectrum: (*a*) MQDT eigenquantum defects as functions of the energy E relative to the double ionisation threshold: ——, 5s*n*s; - - -, 5p*n*p; — —, 4d*n*d (see the text); some experimental levels are indicated by vertical arrows (*n*s means 5s*n*s). (*b*) Lu-Fano plot: ——, theoretical curve $-\nu_s = f(\nu_d)$ or $\tau = f(\nu_d)$; ●, experimental bound levels (Moore 1952, Esherick 1977). Vertical arrows at the top indicate the theoretical $4d^2+5p^2$ and 4d*n*d levels.

of any experimental data this remains a prediction. Additional experimental data are highly desirable to check the reliability of our results.

3.4. Triplet spectra $^3P^o$, $^3D^e$ and $^3S^e$

Channel mixing is generally weaker in the triplet than in the singlet spectra. Below the Sr^+ 5s threshold, the even-parity triplet spectra $^3D^e$ and $^3S^e$ are simpler than the corresponding singlet spectra owing to the absence of $4d^2$ and $5p^2$ states. The number of weakly closed channels required for describing the $^3D^e$ and $^3S^e$ spectra is thus smaller than for the singlets. For each triplet channel, the configurations introduced in expansion (11) are the same as those used for the corresponding singlet channel. Of course, part of these configurations describe strongly closed channels or core relaxation effects, and the corresponding orbitals have zero amplitude at $r = r_0$.

We shall describe each spectrum in succession.

3.4.1. $^3P^o$ spectrum. A two-channel model (5s*n*p, 4d*n*p) is used to describe the perturbation of the 5s*n*p $^3P^o$ series by the 4d5p $^3P^o$ perturber. Figure 6(*a*) shows the MQDT parameters μ_1 (5s*n*p), μ_2 (4d*n*p) and the mixing angle θ as functions of the energy. The energy variation of the parameters is surprisingly large and moreover does not increase monotonically as E increases, in contrast to the $^1P^o$ case. No other theoretical calculation exists for the $^3P^o$ spectra of alkaline earths, prohibiting comparison. Our MQDT parameters at the Sr^+ 5s threshold are instead compared with the empirical ones fitted to the experimental ^3P_J spectra by Armstrong *et al* (1979) (see table 4). As in the $^1P^o$ case, our values are a little smaller than the empirical ones. The comparison between the values of θ bears little significance due to the large energy dependence of the theoretical value, since θ is set constant in the empirical studies. Some theoretical quantum defects and energies are compared with experimental data (Moore 1952, Armstrong *et al* 1979) in table 2 and figure 6(*b*). For clarity, only the $^3P_1$ experimental levels are reported on the Lu-Fano plot. Agreement is good even for the lowest level 5s5p, whose description requires a large energy dependence for μ_1. It should be noted that the 5s5p levels were excluded in previous empirical MQDT analyses (Armstrong *et al* 1979).

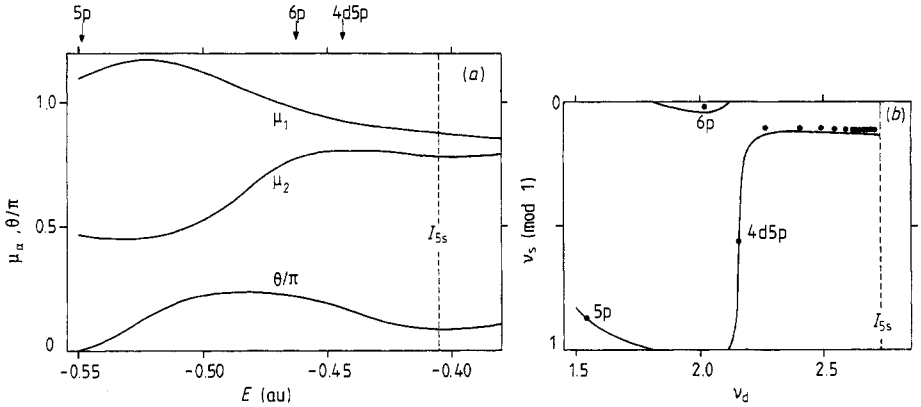

Figure 6. $^3P^o$ spectrum: (*a*) MQDT parameters μ_α and θ as functions of the energy E (see the caption of figure 1(*a*)). (*b*) Lu-Fano plot: ——, theoretical curve; ●, experimental levels (Moore, 1952, Armstrong 1979) (*n*p means 5s*n*p).

Table 4. MQDT parameters for $^3P^o$, $^3D^e$ and $^3S^e$ spectra at the Sr^+ 5s threshold.

			This work			Previous works				
Spectra			μ_1	μ_2	θ/π	Level	μ_1	μ_2	θ/π	Reference
$^3P^o$	1	5s*n*p	0.875	0.784	0.090	$^3P_0$	0.900	0.810	0.146	a
						$^3P_1$	0.896	0.810	0.135	
	2	4d*n*p				$^3P_2$	0.887	0.810	0.138	
						^3P	0.88	0.80	0	b
$^3D^e$	1	5s*n*d	0.722	0.303	0.069	$^3D_1$	0.775	0.322	0.074	c
	2	4d*n*s				$^3D_3$	0.774	0.299	0.073	
						^3D	0.90			
$^3S^e$		5s*n*s	0.347			^3S	0.34			b

[a] Armstrong *et al* (1979).
[b] Armstrong *et al* (1981).
[c] Beigang and Schmidt (1983).

3.4.2. $^3D^e$ spectrum. A two-channel calculation (5s*n*d, 4d*n*s) has been performed to describe the perturbation of high-lying 5s*n*d $^3D^e$ levels by the 4d6s $^3D^e$ level. The energy variation of the MQDT parameters, displayed in figure 7(*a*), is very regular and the channel mixing is very small as expected. Our values of μ_α and θ are in good agreement with those values fitted to the experimental $^3D_1$ and $^3D_3$ spectra by Beigang and Schmidt (1983). However, as in the $^1D^e$ spectrum, μ_1 is a little too small (see table 4). However, this value agrees better with experiment than the *ab initio* value previously obtained by Armstrong *et al* (1979) neglecting channel mixing. Theoretical energies and quantum defects correctly reproduce experimental data (Moore 1952, Esherick 1977, Beigang *et al* 1983) (see figure 7(*b*) and table 2), although the moderately excited 5s*n*d levels lie too high. Here again, the influence of the 4d6s level is distributed over many high-lying 5s*n*d levels with a maximum admixture of 10% in the 5s17d level; Esherick (1977) found a maximum of 8% for the same level.

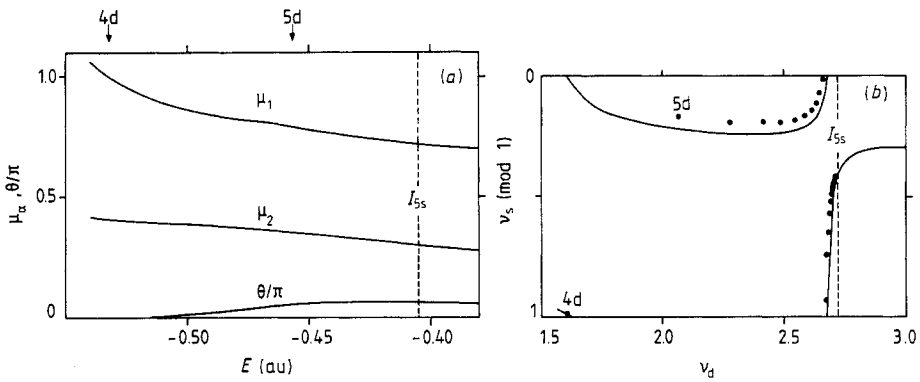

Figure 7. $^3D^e$ spectrum: (*a*) MQDT parameters μ_α and θ as functions of the energy E (nd means 5snd). (*b*) Lu-Fano plot: ——, theoretical curve; ●, experimental $^3D_2$ levels (Moore 1952, Esherick 1977).

3.4.3. $^3S^e$ *spectrum.* For completeness, we have also calculated the quantum defects of the 5sns $^3S_1$ series which is unperturbed below the first ionisation limit. The theoretical energies and quantum defects are compared with experiment in table 2 (Moore 1952, Beigang *et al* 1983). The energy dependence of the quantum defects reproduces the experimental trend well although the eigenquantum defect is a little smaller at threshold, as for all 5snl series.

4. Conclusion

We have shown that the eigenchannel R-matrix method provides reliable data as well as a deeper understanding of the effects of channel mixing in Sr. The various questions previously raised by the empirical MQDT analyses of Sr have been answered. The irregular behaviour of the 4dnp autoionisation lines as n increases has been explained as due to the mixing with 5pns, 5pnd and 4dnf channels. The controversy about the identification of the low-lying perturbers of the $^1D_2$ and $^1S_0$ principal Rydberg series has been resolved, leading to the confirmation of the previous MCHF calculations.

The systematics of channel mixing among the alkaline earths has been analysed. The close similarity between the msnp-mpns $^1P^o$ mixing in light alkaline earths and the 5snp-4dnp mixing in Sr has been demonstrated, at least below the Sr^+ 5s threshold. In contrast, the systematics for channel mixing in the even-parity spectra is less clear; the heavy alkaline earths differ from the lighter ones because of the strong pp-dd mixing.

This paper has demonstrated that the R-matrix used in the light alkaline earths also provides a simple and direct method for obtaining accurate results in Sr. However, the basis for the expansion of the two-electron wavefunctions is larger in Sr than in Be and Mg. The 4dnl channels can be described accurately only by introducing two 4d orbitals: a 4d orbital corresponding to Sr^+ which allows the description of correlation in the asymptotic region, and a 4d′ relaxed orbital corresponding to the neutral atom accounting for the core relaxation effects that are essential in the reaction region. Moreover, the mixing of the 5snl channel with various channels converging towards excited thresholds is important even below the first ionisation limit where most of these channels are strongly closed. This short-range effect is accounted for by the superposition of a large number of nl_1ml_2 configurations in the wavefunction expansion (11).

A similar study might be carried out for Ca. The analysis of the corresponding even-parity singlet spectra is of particular interest since the labelling of some levels is not clear. Moreover, for both Sr and Ca the even-parity spectra are largely unknown and theoretical as well as experimental investigations are thus very desirable.

Some extension of this work would be of great interest. The inclusion of spin-orbit interaction would be very useful. In short range, electrostatic interactions are supposed to prevail over spin-orbit effects. Thus, in a first step, it is possible to completely neglect the spin-orbit effects in the reaction region. By describing the dissociation channels in the pure *jj* coupling scheme, long-range spin-orbit effects could be accounted for using the frame transformation introduced by Lu and Fano (Lu 1971, Lee and Lu 1973, Fano 1975); this consists in constructing the orthogonal transformation $U_{i\alpha}$ between the dissociation channels i in the pure *jj* coupling scheme and the eigenchannels α by using an intermediate set of channels $\bar{\alpha}$ defined in the pure *LS* coupling scheme and the known (*jj*-*LS*) transformation. However, such a simplified approach requires the analysis of the channels described by the same parity and the same J value independently of the *LS* term. The number of interacting channels increases rapidly. For example, the autoionising $J=1$ odd-parity spectrum of Sr below the Sr^+ 4d threshold involves 13 channels of $^1P_1$, $^3P_1$ and $^3D_1$. The introduction of spin-orbit effects in the analysis of this spectrum is expected to improve the description of the 4dnf resonances and the corresponding study is in progress.

At a deeper level, the spin-orbit interaction would not be considered only as resulting in a change of the coupling scheme but would be explicitly introduced in the Hamiltonian and thus in the eigenvalue problem giving the normal logarithmic derivative of the wavefunction on the surface S. The corresponding treatment would certainly be required for analysing channel coupling in Ba.

Another extension concerns the analysis of high-lying doubly-excited states. As the energy increases, the channel mixing becomes more important because larger manifolds of quasidegenerate states become available to the electrons, permitting them to exchange angular momenta and radial kinetic energy more readily. Consequently, channels converging onto more highly excited states, even if strongly closed, have a large cumulative effect which cannot be neglected when the theoretical predictions are required. Furthermore, the size of the reaction volume V increases rapidly when enclosing the charge distribution of excited states of Sr^+. Thus the number of basis functions describing a single channel becomes larger. The complexity of the problem increases rapidly and much exploratory work may well be needed before undertaking a reliable calculation.

Acknowledgment

The authors are grateful to Professor Fano for suggesting this problem and to Professor Greene and Doctor O'Mahony for helpful discussions. Most of the computation was performed at the CIRCE-CNRS, Orsay.

References

Armstrong J A, Jha S S and Pandey K C 1981 *Phys. Rev.* A **23** 2761
Armstrong J A, Wynne J J and Esherick P 1979 *J. Opt. Soc. Am.* **69** 211

Aspect A, Bauche J, Fonseca A L A, Grangier P and Roger G 1984 *J. Phys. B: At. Mol. Phys.* **17** 1761
Aymar M 1984 *Phys. Rep.* **110** 163
Aymar M, Debarre A and Robaux O 1980 *J. Phys. B: At. Mol. Phys.* **13** 108
Beigang R, Lücke K, Schmidt D, Timmermann A and West P J 1983 *Phys. Scr.* **26** 183
Beigang R and Schmidt D 1983 *Phys. Scr.* **27** 172
Cavagnero M 1984 *Phys. Rev.* A **30** 1169
Connerade J P, Baig M A, Garton W R S and Newsom G H 1980 *Proc. R. Soc.* A **371** 295
Cowan R D 1981 *The Theory of Atomic Structure and Spectra, Los Alamos series in basic and applied sciences* (Berkeley, CA: University of California Press)
Esherick P 1977 *Phys. Rev.* A **15** 1920
Ezra G S and Berry R S 1983 *Phys. Rev.* A **28** 1974
Fano U 1975 *J. Opt. Soc. Am.* **65** 979
—— 1983 *Rep. Prog. Phys.* **46** 97
Fano U and Rau A R 1986 *Atomic Collisions and Spectra* (New York: Academic)
Froese Fischer C and Hansen J E 1981 *Phys. Rev.* A **24** 631
—— 1985 *J. Phys. B: At. Mol. Phys.* **18** 4031
Garton W R S and Codling K 1968 *J. Phys. B: At. Mol. Phys.* **1** 106
Garton W R S, Grasdalen G L, Parkinson W H and Reeves E M 1968 *J. Phys. B: At. Mol. Phys.* **1** 114
Greene C H 1981 *Phys. Rev.* A **23** 661
—— 1983 *Phys. Rev.* A **28** 2209
Greene C H, Fano U and Strinati G 1979 *Phys. Rev.* A **19** 1485
Griffin D C, Andrew K L and Cowan R D 1969 *Phys. Rev.* **177** 62
Hahn Y, O'Malley T F and Spruch L 1962 *Phys. Rev.* **128** 932
Hansen J E and Persson W 1977 *J. Phys. B: At. Mol. Phys.* **10** L363
Herrick D R, Kellman M E and Poliak R D 1980 *Phys. Rev.* A **22** 1517
Hudson R D, Carter V L and Young P A 1969 *Phys. Rev.* **180** 77
Krause J L and Berry R S 1985 *J. Chem. Phys.* **83** 5153
Lee C M and Lu K T 1973 *Phys. Rev.* A **8** 1241
Lin C D 1974 *Phys. Rev.* A **10** 1986
—— 1983 *J. Phys. B: At. Mol. Phys.* **16** 723
Lu K T 1971 *Phys. Rev.* A **4** 579
—— 1974 *J. Opt. Soc. Am.* **64** 706
—— 1977 *Proc. R. Soc.* A **353** 431
Macek J H 1966 *Phys. Rev.* **146** 50
Manson S T 1969 *Phys. Rev.* **182** 97
Moore C E 1952 *Atomic Energy Levels* NBS Circular no 467 vol 2 (Washington, DC: US Govt Printing Office) p 14
Newsom G H, O'Connor S O and Learner R C M 1973 *J. Phys. B: At. Mol. Phys.* **6** 2162
O'Mahony P F 1985 *Phys. Rev.* A **32** 908
O'Mahony P F and Greene C H 1985 *Phys. Rev.* A **31** 250
O'Mahony P F and Watanabe S 1985 *J. Phys. B: At. Mol. Phys.* **18** L239
Parkinson W H, Reeves E M and Tomkins F S 1976 *J. Phys. B: At. Mol. Phys.* **9** 157
Percival I C 1960 *Phys. Rev.* **119** 159
Robaux O and Aymar M 1982 *Comput. Phys. Commun.* **25** 223
Seaton M J 1983 *Rep. Prog. Phys.* **46** 167
Watanabe S and Lin C D 1986 *Phys. Rev.* A **34** 823
Wynne J J and Armstrong J A 1979 *IBM J. Res. Dev.* **23** 490